2002 INTERNATIONAL CONFERENCE ON
METAL POWDER DEPOSITION FOR RAPID MANUFACTURING
April 2002, San Antonio, Texas, USA

SIMULATION OF LAYER OVERLAP TEMPERING KINETICS IN STEEL PARTS DEPOSITED BY LASER CLADDING

L. Costa[1], T. Reti[2], A. M. Deus[1], R. Vilar[1]

[1] Instituto Superior Técnico, Dep. Eng. Materiais, Av. Rovisco Pais, 1049-001 Lisboa, Portugal
[2] Budapest Polytechnic, H-1081 Budapest, Népszínház u. 8., Hungary

ABSTRACT

The application of laser cladding in multiple-layer deposition processes to build complex metal parts is attracting considerable attention. Due to the fast cooling rates in laser cladding, diffusive solid-state transformations are normally suppressed, but as successive clad tracks are overlapped, the associated thermal input is driven by heat conduction to the previously deposited layers. These layers undergo a succession of anisothermal cycles that may lead to complex phase transformations. In steels, in particular, decomposition of the metastable phases present in the material will occur. Some of these phase transformations produce changes in the material specific volume, promoting residual stress-induced deformation or even cracking of the part. Also, the properties of the deposited material are progressively modified as thermal cycles are overlapped. In this paper, the solid state phase transformations in tool steels deposited by laser metal powder deposition are modelled. Kinetic models describing non-isothermal tempering of martensite were coupled with a heat transfer model to simulate the tempering effects that result from the successive overlap of clad layers.

INTRODUCTION

Laser metal powder deposition of tool steels is finding significant application in rapid tooling [1-4]. Besides building fully dense steel parts with complex geometric features, the deposited materials must exhibit properties that comply with the intended application requirements. The chemical composition, solidification microstructure, and subsequent heat treatments applied to the material determine these properties. Due to the fast solidification and cooling rates, the laser processed tool steels may contain significant amounts of metastable phases, in particular of austenite and martensite [5]. The volume fractions of these phases depend on the processing parameters and even on the amount of material deposited in each layer. Niu et. al. [6] have deposited AISI M2 high-speed steel and reported a decrease in the proportion of retained austenite, accompanied by an increase of the amount of carbides, as the clad layer thickness is increased. As the layer overlapping process is carried out, the previously deposited material will undergo a periodic anisothermal tempering cycle that, depending on the temperature reached, will activate several diffusional transformations that lead to the decomposition of the metastable phases,

progressively changing the material microstructure and properties [7]. The deposition strategy used to build a certain metal part determines the temperature field, which, together with the kinetics of the transformations that may occur in the material, defines the final properties of the material. To simulate the effects of these thermal cycles, a simple three-dimensional thermo-kinetic finite element model has been implemented. The volume fraction of martensite resulting from the transformation of austenite is evaluated using the Koistinen-Marburger equation [8], while the tempering intensity is estimated with the Dorn parameter [9,10].

This model has been applied to the deposition of AISI P20 tool steel (0.40% C, 1.50% Mn, 0.35% Si, 1.90% Cr, 0.20% Mo) that, in the quenched and tempered condition, is used in zinc die casting dies and plastic molds. The values of the relevant material properties used in the calculations are summarised in table 1. A time-temperature-transformation (TTT) diagram (figure 1) for P20 steel shows the microstructures to expect according to the cooling path.

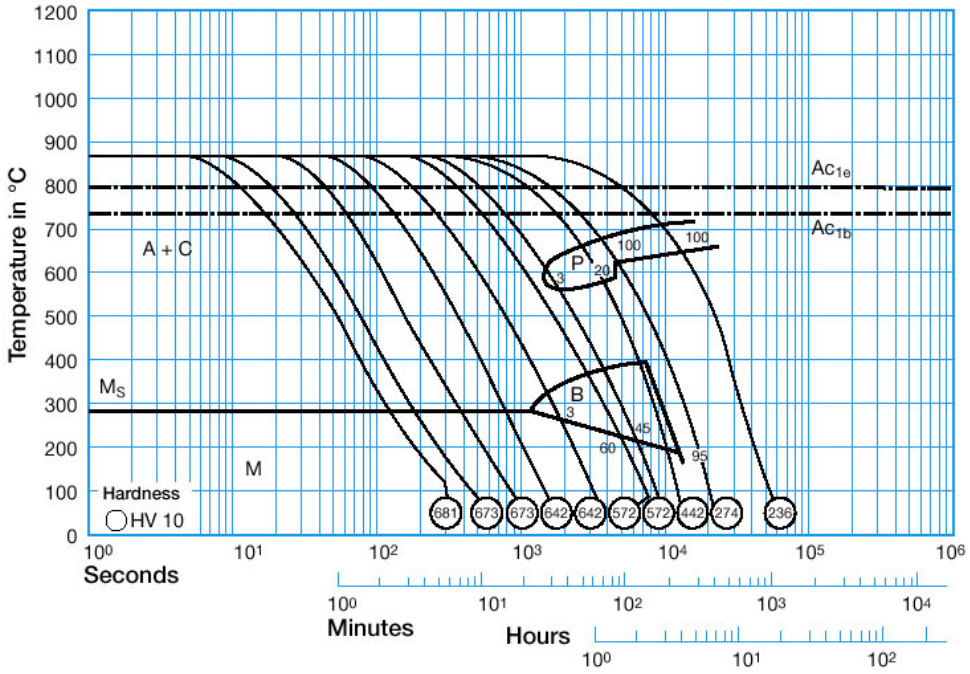

Figure 1. TTT diagram for AISI P20 tool steel [11].

Table 1. Material properties used to simulate laser deposition of AISI P20 tool steel [12].

Thermal conductivity			Specific heat			Density	
Phase	Temp. (ºC)	K (W/m/K)	Phase	Temp. (ºC)	C_p (J/kg/K)	Temp. (ºC)	ρ (kg/m^3)
Austenite	20	12.0	Austenite	400	550	20	7800
Austenite	900	26.8	Austenite	600	550	200	7750
Austenite	1100	28.9	Austenite	900	600	400	7700
Austenite	1300	32.8	Austenite	1300	750		
Austenite	1458	34.0	Martensite	20	460		
Martensite	20	29.0	Latent heat released during solidification: 250 kJ/kg				
Martensite	200	29.5					
Martensite	400	31.0					

THE THERMO-KINETIC MODEL

In laser metal powder deposition of tool steels, the cooling rates are high and, in general, it is assumed that after complete cooling the material is completely martensitic. However, Colaço et. al. [5] have shown that, under certain conditions, amounts of retained austenite as high as 100% can appear, probably due to the inhibition of the martensitic transformation by the very fine austenitic grain size. On the other hand, since austenitisation is determined by the time-temperature cycle above the eutectoid temperature (A1), the rapidly varying and non-uniform temperature field produced by a laser beam can produce incomplete austenitisation, affecting the formation of martensite [13]. These phenomena have not been included in the present model. It is assumed that, after solidification, the deposited material transforms into homogeneous austenite and that, when martensite is heated above 800 ºC, it also transforms into homogeneous austenite. Austenite starts to transform into martensite as the temperature drops below the martensite start temperature, Ms. The volume fraction, f, of martensite is given by the Koistenen-Marburger equation [8]:

$$f = 1 - \exp(-1.10\times10^{-2} \cdot \Delta T), \tag{1}$$

and it depends only on the undercooling, ΔT, below the Ms temperature. The Ms temperature is related with the steel chemical composition by the Andrews equation [14]:

$$Ms\ (^{\circ}C) = 539 - 423C - 30.4Mn - 12.1Cr - 7.5Mo - 7.5Si\ , \tag{2}$$

where the element designations refer to concentrations in wt%. For P20, Ms = 297 ºC.

Martensite in Fe-C alloys and steels is a supersaturated unstable phase that decomposes when heated (martensite tempering) [7]. During this process, several diffusional transformations (activated at different temperatures) will progressively change the microstructure of the material, affecting properties such as hardness, strength, and toughness [15]. Thus, as material layers are overlapped, a change in properties can be expected to occur provided that the transformation kinetics of those reactions are sufficiently rapid for a significant transformation to occur during the short thermal cycles characterising the laser metal powder deposition process. The evolution of the microstructure and material properties due to thermally activated metallurgical processes is described by the (isothermal) transformation kinetics [7]. The formal generalisation of these functions to describe non-isothermal processes [10] involves the definition of time-temperature dependent parameters, which unambiguously characterise the progress of the process taking place. For instance, the Dorn parameter P_D [9] uses the Arrhenius equation to evaluate the temperature-dependent transformation rate and is valid for describing steel tempering under anisothermal conditions [10]:

$$P_D = \int_0^t e^{-Q/RT} \cdot dt\ , \tag{3}$$

where Q represents the process activation energy, R the universal gas constant, and T the temperature. The hardness of the material is commonly used to characterise the extent of tempering. The kinetic equation [10] describing the change in hardness of steel tempered in continuously changing temperature conditions is of the form:

$$H = H_0 + A(P_D)^n\ , \tag{4}$$

where H_0 is the as-quenched hardness, A and n are constants, and P_D is the Dorn parameter, which accounts for the combined influence of time and temperature. Data obtained from isothermal tempering experiments [11,12] are used to determine the values of A, n, and Q by regression analysis, based on the method of least squares. The hardness of quenched AISI P20 steel, tempered at different temperatures during 2 hours and 2 + 2 hours is given in figure 2.

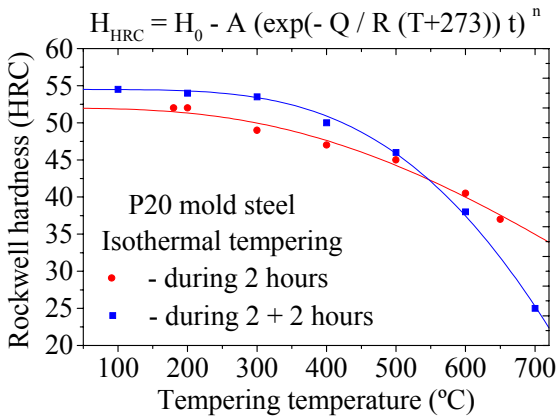

Figure 2. Tempering response of P20 steel.

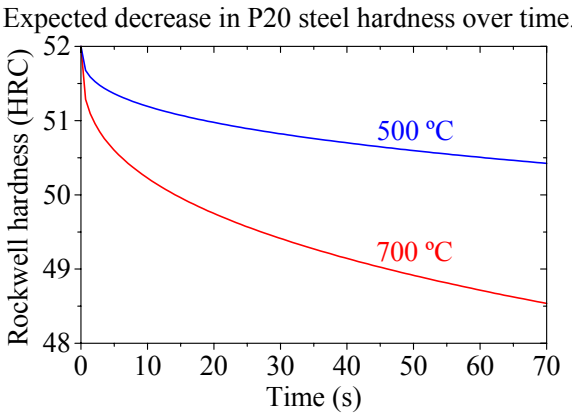

Figure 3. Decrease in hardness over time.

To describe the change in the hardness distribution as consecutive layers of material are overlapped, eq. 4 was fit to the experimental isothermal data (figure 2), assuming that the activation energy is similar for both tempering processes. The Rockwell hardness of as-quenched AISI P20 steel, tempered at a constant temperature T (in Kelvin) during time interval t (in seconds) is given by

$$H_{HRC} = 52 - 16.8632 (\exp (-71619 / 8.314 (T + 273)) t)^{0.34379} . \quad (5)$$

Using the previous result, the expected hardness decrease occurring during layer overlap tempering by laser metal powder deposition of AISI P20 tool steel has been estimated and is presented in figure 3.

The martensite formation (eq. 1) and tempering (eq. 5) processes described previously have been combined to simulate the non-isothermal tempering that results from overlapping successive layers of material. Using a commercial finite element analysis software package [16], a heat transfer model has been coupled with the phase transformation kinetics equations. It was assumed that complete austenitisation occurs if the temperature exceeds 800 ºC, that the martensitic transformation starts when the temperature drops below the Ms temperature, and that the tempered martensite hardness change is described by the Dorn parameter. Laser powder deposition has been previously modelled using finite element analysis to study thermally induced residual stress fields [17-21] and solidification [22-24]. In some cases [17,24] the material deposition was modelled by adding groups of cubic elements step-by-step. Given the material density, clad track width (1 mm), scanning speed (20 mm/s), powder feed rate (0.1 g/s) and the linear dimension of the individual cubic elements (0.5 mm), the number of elements (2×1×2) added in each time step (0.05 s) was calculated by considering a powder use efficiency of 78% (figure 4).

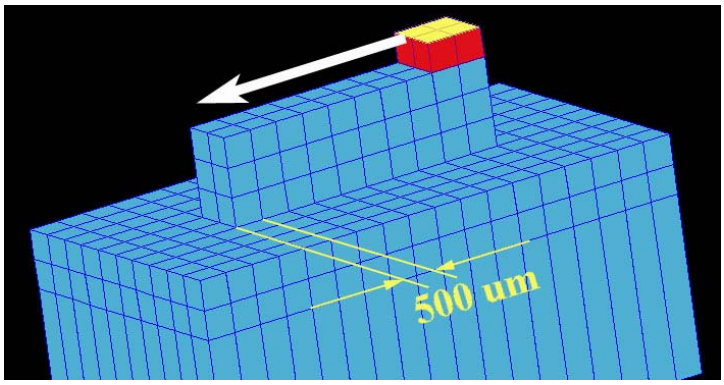

Figure 4. Build-up of a wall structure. In each individual time step of 0.05 seconds, a group of 4 cubic elements (red) are added to the previously deposited material (blue). The white arrow indicates the deposition direction.

A total of eight layers, each with a length of 5.0 mm, 0.5 mm height and 1.0 mm width, were overlapped in the same direction over a large substrate of the same material, acting as a heat sink. All elements with exposed surfaces undergo heat loss by convection and radiation. The initial temperature of the added elements (red in figure 4) is 1500 ºC [25] and these elements are irradiated (through the top surfaces) by a moving Gaussian laser beam with a power of 1900 W focused into a spot with 3 mm diameter. During each time step, the material properties of each element are calculated as a weighed average of the properties of the individual phases (table 1), by considering the phase fractions present. The latent heat [26] associated to the phase transformations occurring during martensite tempering has been neglected in the model. To study the influence of the deposition strategy two different time delays, Δt, separating the overlapping of consecutive layers, were used to simulate the build-up of a thin wall structure.

RESULTS AND DISCUSSION

The time interval over which the experiments illustrated in figures 5 to 7 occur implies that the cooling rate is high enough to avoid the austenite perlitic and bainitic transformations (see figure 1). As a result, only martensite may form. The calculated temperature field (figure 5), phase volume fractions (figure 6) and final hardness (figure 7) are shown below. The elapsed time since the beginning of the experiment is indicated by t_{STEP}.

a) t_{STEP} = 5.5 seconds, Δt = 0.5 seconds

b) t_{STEP} = 37.0 seconds, Δt = 5.0 seconds

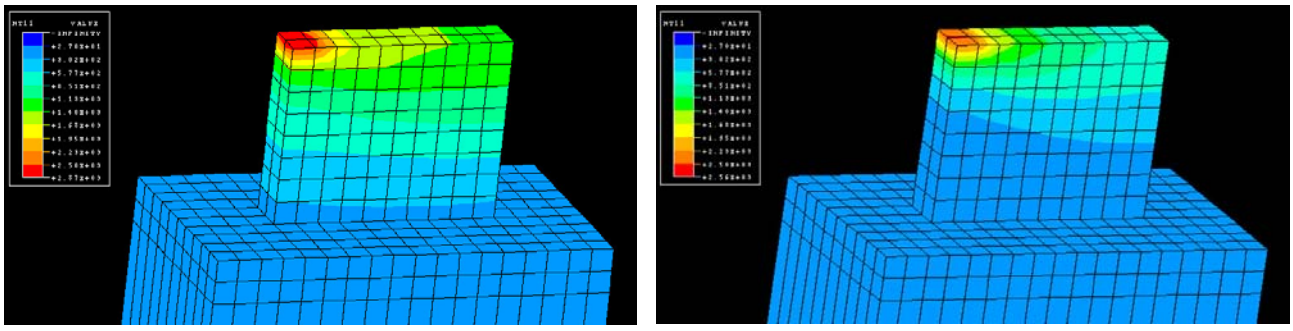

Figure 5. Temperature field at the end of the last deposition step.
27 ºC - blue; 2500 ºC – red

a) t_{STEP} = 5.5 seconds, Δt = 0.5 seconds

b) t_{STEP} = 37.0 seconds, Δt = 5.0 seconds

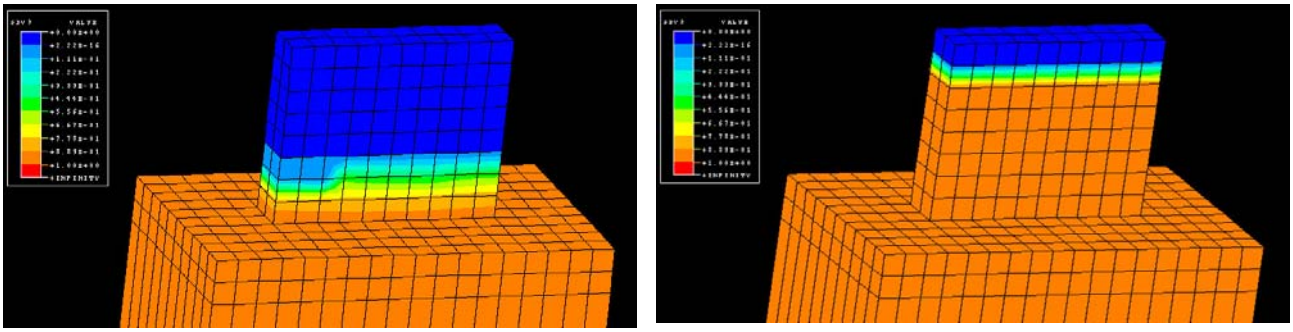

Figure 6. Phase map at the end of the last deposition step.
100% Martensite – red; 100 % Austenite – blue

a) t_{STEP} = 16.0 seconds, Δt = 0.5 seconds

b) t_{STEP} = 52.0 seconds, Δt = 5.0 seconds

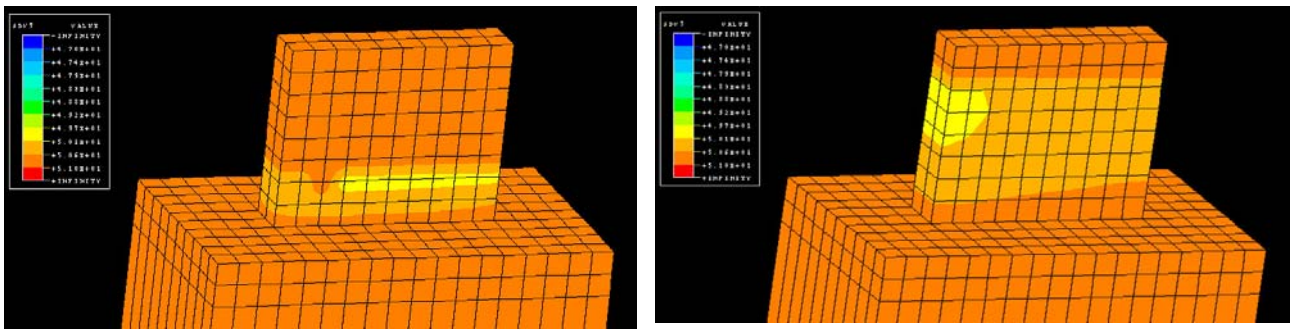

Figure 7. Final hardness distribution, after cooling down to room temperature.
52 HRC – red; 50 HRC – yellow

As the thin wall is deposited, the resulting thermal field is critically affected by the time delay Δt (figures 5 a) and b)). If Δt is small, the deposited material does not have enough time to cool down below the Ms temperature before the addition of the next layer. As a result, heat builds up in the material and the temperature remains higher than Ms, hence the martensitic transformation does not occur and a significant region of the deposited material remains austenitic (figure 6 a)). Only the material close to the substrate cools down enough to form martensite. If Δt is sufficiently large, each layer of the deposited material will cool down below Ms before the addition of a new layer, and the material in that layer transforms into martensite (figure 6 b)). Subsequently, this martensite undergoes tempering, as successive clad tracks are added. As martensite decomposes, the material properties change. When Δt is sufficiently large the deposited material undergoes repeated tempering and its hardness decreases continuously as the wall height increases (figure 7 b)). If Δt is small, a noticeable change in hardness will only be observed in a narrow region of the wall close to the substrate (figure 7 a)), because elsewhere the material remains austenitic and tempering transformations do not occur. Therefore, depending on the Δt value, the tempering effects may be located only in the first deposited tracks, or may be more evenly distributed along the wall height. Besides Δt, the properties of the deposited steel will depend on other parameters such as the processing speed: if the wall is built-up at low scanning speed, the successive thermal cycles affecting martensite will last longer, enhancing the tempering effects.

CONCLUSIONS

A simple three-dimensional thermo-kinetic finite element model has been implemented to simulate the austenite to martensite transformation and the martensite tempering, which occur as successive layers of material are overlapped in laser metal powder deposition processes. Depending on the deposition strategy, changes in the material properties can be concentrated close to the base material or can be uniformly distributed along the height of the deposited structure. A short time delay separating the overlap of successive layers temporarily inhibits the austenite to martensite transformation during the part build up. This transformation will only occur after the deposition process has ended, when the whole structure cools down below the martensite start temperature. In this case, significant tempering will only be observed in the first deposited layers, located close to the base material. A large time delay between successive layers allows the deposited material to transform to martensite before the next deposition step. Gradually, the overlapping heat cycles temper the lower layers and changes in the material properties are uniformly distributed along the height of the deposited structure. Changes in the material properties due to layer overlap tempering can be reduced if the steel presents a sluggish decomposition kinetics.

REFERENCES

[1] R. Vilar, "Laser Cladding", *Inter. J. Powder Metall.*, Vol. 37, No. 2, 2001, pp. 31-48.
[2] J.W. Sears, "Solid freeform fabrication technologies: rapid prototyping - rapid manufacturing", *Inter. J. Powder Metall.*, Vol. 37, No. 2, 2001, pp. 29-30.
[3] D. Morgan, "New metal-fabrication application", *Industrial Laser Solutions*, Vol. 15, No. 1, 2000, pp. 8-10.
[4] O. Graydon, "Jets of molten metal make industrial parts", *Opto & Laser Europe*, No. 47, 1998, pp. 33-35.
[5] R. Colaço and R. Vilar, "Effect of the processing parameters on the proportion of retained austenite in laser surface melted tool steels", *J. Mater. Sci. Lett.*, Vol. 17, No. 1998, pp. 563-567.
[6] H.J. Niu and I.T.H. Chang, "Microstructural evolution during laser cladding of M2 high-speed steel", *Metall. Mater. Trans.*, Vol. 31A, No. 10, 2000, pp. 2615-2625.
[7] D.A. Porter and K.E. Easterling, *Phase transformations in metals and alloys*, Chapman & Hall, London, UK, 1992.
[8] D.P. Koistinen and R.E. Marburger, "A general equation prescribing the extent of the austenite-martensite transformation in pure iron-carbon alloys and plain carbon steels", *Acta Metall.*, Vol. 7, 1959, pp. 59-60.
[9] O.D. Sherby, J.L. Lytton and J.E. Dorn, "Activation energies for creep of high-purity aluminum", *Acta Metall.*, Vol. 5, 1957, pp. 219-227.
[10] T. Réti, G. Bobok and M. Gergely, "Computing method for non-isothermal heat treatments", *International Conference Heat Treatment '81*, The Metals Society, Birmingham, 1981, p. 91.
[11] Edelstahl Witten-Krefeld GmbH. (2002). *Steels for Plastic Moulding*. http://www.edelstahl-witten-krefeld.de/e_werkst/kunst.html.
[12] Edro Specialty Steels. (2002). *Prehardened mold quality P20*. http://www.edro.com/edro3.html.
[13] T. Réti, G. Bagyinszki, I. Felde, B. Vero and T. Bell, "Prediction of as-quenched hardness after rapid austenitization and cooling of surface hardened steels", *Comp. Mater. Sci.*, Vol. 15, 1999, pp. 101-112.
[14] K.W. Andrews, "Empirical formulae for the calculation of some transformation temperatures", *JISI*, Vol. 203, 1965, pp. 721-727.
[15] *Metals Handbook*, Vol. 1, ASM International, Metals Park, OH, USA, 1990, p. 705.
[16] Hibbitt, Karlsson & Sorensen, Inc., *ABAQUS manual*, Pawtucket, RI, USA, 1999.
[17] K. Dai and L. Shaw, "Thermal and stress modeling of multi-material laser processing", *Acta Mater.*, Vol. 49, 2001, pp. 4171-4181.
[18] A. Vasinonta, J. Beuth and M. Griffith, "Process maps for laser deposition of thin-walled structures", *Solid freeform fabrication Symposium*, compiled by D. Bourell, J. Beaman, R. Crawford, H. Marcus and J. Barlow, The University of Texas at Austin, 1999, p. 383.
[19] A. Vasinonta, J. Beuth and M. Griffith, "Process maps for controlling residual stress and melt pool size in laser-based SFF processes", *Solid freeform fabrication Symposium*, compiled by D. Bourell, J. Beaman, R. Crawford, H. Marcus and J. Barlow, The University of Texas at Austin, 2000, p. 200.
[20] A.M. Deus and J. Mazumder, "Two-dimensional thermo-mechanical finite element model for laser cladding", *ICALEO'96*, Vol. 81, compiled by W. Duley, K. Shibata and R. Poprawe, Laser Institute of America, 1996, p. B/174.
[21] A.H. Nickel, D.M. Barnett and F.B. Prinz, "Thermal stresses and deposition patterns in layered manufacturing", *Mater. Sci. Eng.*, Vol. A317, 2001, pp. 59-64.
[22] A.F.A. Hoadley and M. Rappaz, "A thermal model of laser cladding by powder injection", *Metall. Trans.*, Vol. 23B, 1992, pp. 631-642.
[23] M. Picasso and M. Rappaz, "Laser-powder-material interactions in the laser cladding process", *J. Physique IV*, Vol. 4, 1994, pp. C4/27-33.
[24] W. Hofmeister, M. Wert, J. Smugeresky, J. Philliber, M. Griffith and M. Ensz. (1999). *JOM-e, Vol. 51, No. 7: Investigating solidification with the Laser-engineered net shaping (LENS) process*. http://www.tms.org/pubs/journals/JOM/9907/Hofmeister/Hofmeister-9907.html.
[25] O.O.D. Neto and R. Vilar, "Physical-computational model to describe the interaction between a laser beam and a powder jet in laser surface processing", *J. Laser Appl.*, Vol. 14, No. 1, 2002, pp. 46-51.

[26] L. Cheng, C.M. Brakman, B.M. Korevaar and E.J. Mittemeijer, "The tempering of iron-carbon martensite; dilatometric and calorimetric analysis", *Metall. Trans.*, Vol. 19A, No. 10, 1988, pp. 2415-2426.